iScience

CellPress
OPEN ACCESS

Article

Predicting left ventricular remodeling post-MI through coronary physiological measurements based on computational fluid dynamics

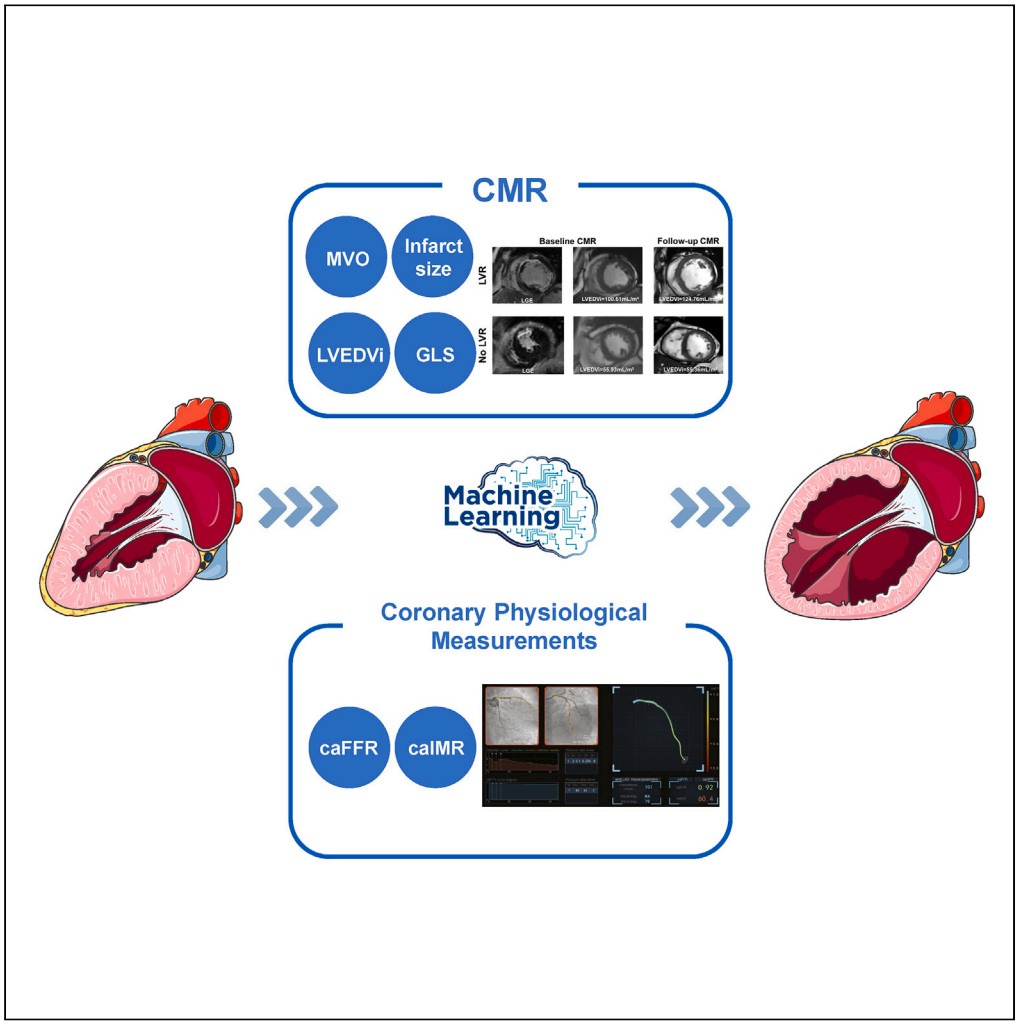

Wen Zheng, Qian Guo, Ruifeng Guo, ..., Bin Que, Xiao Wang, Shaoping Nie

xwang@mail.ccmu.edu.cn (X.W.)
spnie@ccmu.edu.cn (S.N.)

Highlights

Larger infarcts, MVO, and lower caFFR predict a higher likelihood of LVR

Machine learning enhanced LVR prediction with CMR or coronary physiology parameters

Coronary physiology offers a more convenient approach than CMR for predicting LVR

Machine learning identified several key risk factors for LVR

Zheng et al., iScience 27, 109513
April 19, 2024
https://doi.org/10.1016/j.isci.2024.109513

iScience

CellPress
OPEN ACCESS

Article

Predicting left ventricular remodeling post-MI through coronary physiological measurements based on computational fluid dynamics

Wen Zheng,[1,4] Qian Guo,[1,4] Ruifeng Guo,[1] Yingying Guo,[1] Hui Wang,[2] Lei Xu,[2] Yunlong Huo,[3] Hui Ai,[1] Bin Que,[1] Xiao Wang,[1,5,*] and Shaoping Nie[1,*]

SUMMARY

Early detection of left ventricular remodeling (LVR) is crucial. While cardiac magnetic resonance (CMR) provides valuable information, it has limitations. Coronary angiography-derived fractional flow reserve (caFFR) and index of microcirculatory resistance (caIMR) offer viable alternatives. 157 patients with ST-segment elevation myocardial infarction (STEMI) undergoing primary percutaneous coronary intervention were prospectively included. 23.6% of patients showed LVR. Machine learning algorithms constructed three LVR prediction models: Model 1 incorporated clinical and procedural parameters, Model 2 added CMR parameters, and Model 3 included echocardiographic and functional parameters (caFFR and caIMR) with Model 1. The random forest algorithm showed robust performance, achieving AUC of 0.77, 0.84, and 0.85 for Models 1, 2, and 3. SHAP analysis identified top features in Model 2 (infarct size, microvascular obstruction, admission hemoglobin) and Model 3 (current smoking, caFFR, admission hemoglobin). Findings indicate coronary physiology and echocardiographic parameters effectively predict LVR in patients with STEMI, suggesting their potential to replace CMR.

INTRODUCTION

Left ventricular remodeling (LVR) refers to the changes in left ventricular size, shape, structure, and function that occur in response to injury, such as myocardial infarction (MI). It is an important prognostic factor that continues to affect nearly half of the patients with ST-elevated myocardial infarction (STEMI), despite advancements such as percutaneous coronary intervention (PCI) and optimal medical therapy.[1–3] LVR following MI can lead to hypertrophy, heart failure, arrhythmias, and sudden cardiac death. Therefore, the early identification of LVR is crucial due to its association with heart failure and cardiac mortality.[2,4,5]

Traditionally, relying on clinical factors for the risk stratification of LVR has limitations. However, cardiac magnetic resonance (CMR) imaging has provided valuable insights into the cardiac structure and function related to MI. Several imaging modalities have shown predictive capabilities for ventricular remodeling.[6,7] Myocardial strain has proven more sensitive than left ventricular ejection fraction (LVEF) as a marker of LVR-related cardiac dysfunction.[8,9] Infarct size (% LV mass with late gadolinium enhancement [LGE]) indicates the extent of irreversibly damaged myocardium and predicts remodeling risk.[10,11] Microvascular obstruction (MVO) and intramyocardial hemorrhage (IMH) signify ischemia-reperfusion injury to the cardiac microvasculature independently predicting adverse remodeling.[12] Despite their value in CMR modalities also have limitations, including long processing times, high costs, and contraindications. Coronary microvascular dysfunction (CMD), caused by factors such as oxidative stress and inflammation can lead to myocardial ischemia affecting the cardiac function prognosis in patients with STEMI.

CMD, caused by factors such as oxidative stress and inflammation can lead to myocardial ischemia affecting the cardiac function prognosis in patients with STEMI.[13] Both fractional flow reserve (FFR) and the index of microcirculatory resistance (IMR) provide insights into coronary stenosis and microvascular function. However, measuring them during primary PCI in patients with STEMI can be challenging.[14] Non-invasive alternatives such as coronary angiography-derived FFR (caFFR) and IMR (caIMR) help overcome these challenges. caFFR and caIMR utilize computer algorithms that analyze coronary angiography images to facilitate the assessment of coronary lesions and microcirculatory function.[15,16]

[1]Center for Coronary Artery Disease, Department of Cardiology, Beijing Anzhen Hospital, Capital Medical University, Beijing Institute of Heart Lung and Blood Vessel Diseases, Beijing, China
[2]Department of Radiology, Beijing Anzhen Hospital, Capital Medical University, Beijing Institute of Heart Lung and Blood Vessel Diseases, Beijing, China
[3]Institute of Mechanobiology & Medical Engineering, School of Life Sciences & Biotechnology, Shanghai Jiao Tong University, Shanghai, China
[4]These authors contributed equally
[5]Lead contact
*Correspondence: xwang@mail.ccmu.edu.cn (X.W.), spnie@ccmu.edu.cn (S.N.)
https://doi.org/10.1016/j.isci.2024.109513

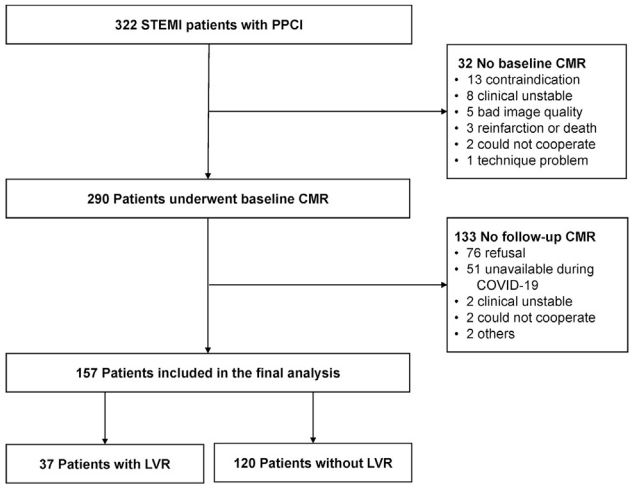

Figure 1. The study flow diagram

Abbreviations: CMR, cardiac magnetic resonance; LVR, left ventricular remodeling; PPCI, primary percutaneous coronary intervention; STEMI, ST-elevation myocardial infarction.

Recent advancements in artificial intelligence and machine learning (ML) have shown potential for early disease detection and risk prediction.[17] ML enables the recognition of complex patterns in data to predict outcomes without being limited by established risk factors. By applying ML models to traditional indices as well as emerging indices derived from coronary angiography, this study aims to overcome CMR challenges in patients with STEMI for the early and practical prediction of LVR risk.

RESULTS

Baseline characteristics

From the 322 patients initially included in our STEMI cohort, 157 for whom we could cross-match our clinical, CMR, and clinical data were finally included in our study (Figure 1). Of those 157 patients, 37 (23.6%) had LVR at three months. The study population's clinical, procedural, and coronary hemodynamic parameters and CMR characteristics are shown in Tables 1 and 2.

Feature selection

In the feature selection process, we used the LASSO regularization and BORUTA to help eliminate features with insufficient information. This process iteratively employed these two feature selection algorithms to reduce the feature number by eliminating features not selected at each iteration by any algorithm. Some stable features from clinical, PCI, echocardiographic parameters, and CMR parameters were finally selected, including sex, age, current cigarette smoking, hemoglobin, HbA1c, treatment with MRA and ACEI or ARB or ARNI, TIMI flow grade post-PCI, the number of stents, caIMR, caFFR, LVEDVi, infarct size, presence of MVO and GLS, and two echocardiographic parameters (LVEF and LVEDD).

Model development and evaluation

The derivation cohort was divided into a 70% training dataset and a 30% testing dataset (the former referred to as the training dataset, the latter as the internal validation or evaluation dataset). The former used four ML algorithms to train and adjust the model parameters. The latter tested the developed model on unseen data (a typical process in ML to verify the model's generalization ability, i.e., the model's ability to correctly classify unseen data).

Three prediction models were constructed to evaluate the incremental discrimination and reclassification performance of clinical, PCI, and CMR parameters in predicting LVR. Model 1 was based on clinical parameters including sex, age, current smoking, hemoglobin, HbA1c, MRA, ACEI, or ARB, or ARNI therapy, and PCI variables such as the number of stents and TIMI flow grade post-PCI. Model 2 added CMR parameters (infarct size, MVO, LVEDVi, and GLS) to Model 1, and Model 3 combined echocardiographic (LVEF and LVEDD) and functional parameters (caIMR and caFFR) with Model 1. The performance of four ML algorithms, XGBoost, KNN, LR, and RF, in constructing LVR prediction models was compared.

The RF algorithm performed well in all three models, with the area under the receiver operating characteristic curve (AUC) values of 0.77 for model 1, 0.84 for model 2, and 0.85 for model 3. The AUC of other models is shown in Figures 2 and S1. Accuracy, sensitivity, and specificity for each model are reported in Table S1. Based on these findings, we chose the RF algorithm as the final prediction model because of its consistently excellent performance in predicting LVR after MI. There were significant differences in AUC between model 1 and model 2 or model 3

Table 1. Baseline characteristics of the study population

	Overall (n = 157)	No remodeling (n = 120)	Remodeling (n = 37)	*p* value
Demographics				
Age, year	57.4 ± 10.9	57.7 ± 11.2	56.6 ± 10.2	0.602
Male	131 (83.4%)	101 (84.2%)	30 (81.1%)	0.659
BMI, kg/m^2	25.9 ± 3.5	25.9 ± 3.5	25.8 ± 3.3	0.892
Current smoker	78 (50.0%)	63 (52.5%)	15 (41.7%)	0.447
Systolic blood pressure, mmHg	122.9 ± 14.5	123.6 ± 14.9	120.5 ± 13.0	0.259
Diastolic blood pressure, mmHg	77.3 ± 9.7	77.1 ± 9.7	78.0 ± 9.9	0.635
Heart rate, beats/min	79.8 ± 12.1	80.1 ± 12.0	79.0 ± 12.6	0.630
Location anterior	97 (61.8%)	68 (56.7%)	29 (78.4%)	0.017
Killip class				0.200
I	104 (66.2%)	78 (65.0%)	26 (70.3%)	
II	47 (29.9%)	39 (32.5%)	8 (21.6%)	
III	2 (1.3%)	1 (0.8%)	1 (2.7%)	
IV	4 (5.4%)	2 (1.7%)	2 (5.4%)	
Blood results				
Peak hs-TnI, ng/mL	26.5 (20.0, 28.5)	26.5 (19.7, 29.2)	27.9 (21.9, 28.0)	0.438
Peak CKMB, ng/mL	196.5 (107.3, 255.0)	194.1 (101.6, 251.8)	211.0 (107.3, 289.2)	0.485
Peak BNP, pg/mL	257.0 (122.5, 436.5)	245.0 (116.8, 429.5)	275.0 (132.0, 497.0)	0.459
Hemoglobin, g/L	150.5 ± 14.2	151.5 ± 14.2	147.2 ± 14.0	0.108
Neutrophil ratio, %	81.2 (70.5, 86.0)	81.0 (70.4, 85.4)	82.4 (71.1, 87.6)	0.222
Fasting blood glucose, mmol/L	7.2 (5.9, 10.0)	6.8 (5.8, 10.6)	7.4 (6.2, 9.6)	0.373
Glycated hemoglobin, %	6.0 (5.5, 7.4)	6.0 (5.5, 7.5)	6.0 (5.6, 7.0)	0.617
eGFR, mL/min/1.73 m^2	108.3 (87.5, 120.6)	108.7 (85.9, 130.0)	108.3 (90.0, 128.8)	0.679
hs-CRP, mg/L	3.2 (1.5, 6.1)	3.3 (1.5, 6.1)	6.5 (2.3, 9.9)	0.027
Angiographic findings				
Total ischemic time, min	285.0 (199.5, 497.5)	286.0 (195.5, 498.8)	285.0 (204.5, 462.5)	0.960
Procedures				
Culprit lesion				0.122
LAD	96 (61.1%)	68 (70.8%)	28 (75.7%)	
RCA	45 (28.7%)	38 (31.7%)	7 (18.9%)	
LCX	16 (10.2%)	14 (11.7%)	2 (5.4%)	
Reperfusion therapy				
Aspiration thrombectomy	74 (47.1%)	55 (45.8%)	19 (51.4%)	0.557
Balloon angioplasty only	10 (6.4%)	6 (5.0%)	4 (10.8%)	0.247
PCI with stent implantation	143 (91.1%)	111 (92.5%)	32 (86.5%)	0.321
Number of stents				0.584
0	14 (8.9%)	9 (7.5%)	5 (13.5%)	
1	112 (71.3%)	88 (73.3%)	24 (64.9%)	
2	26 (16.6%)	19 (15.8%)	7 (18.9%)	
3	5 (3.2%)	4 (3.3%)	1 (2.7%)	
TIMI flow grade pre-PCI				0.921
0	104 (66.2%)	79 (65.8%)	25 (67.6%)	
1	6 (3.8%)	4 (3.3%)	2 (5.4%)	
2	15 (9.6%)	12 (10.0%)	3 (8.1%)	
3	32 (20.4%)	25 (20.8%)	7 (18.9%)	

(*Continued on next page*)

Table 1. *Continued*

	Overall (n = 157)	No remodeling (n = 120)	Remodeling (n = 37)	*p* value
TIMI flow grade post-PCI				0.573
0/1	0 (0.0%)	0 (0.0%)	0 (0.0%)	
2	4 (2.5%)	4 (3.3%)	0 (0.0%)	
3	153 (97.5%)	116 (96.7%)	37 (100.0%)	
GP IIb/IIIa inhibitor	105 (66.9%)	35 (29.2%)	17 (45.9%)	0.058
Medications at discharge				
β blockers	127 (80.9%)	94 (78.3%)	33 (89.2%)	0.142
ACEI/ARB/ARNI	116 (73.9%)	84 (70.0%)	32 (86.5%)	0.046
Diuretic agent	15 (9.6%)	11 (9.2%)	4 (10.8%)	0.766
MRA	28 (17.8%)	20 (16.7%)	8 (21.6%)	0.491
Angiography-derived physiologic indices				
caIMR	26.7 (19.1, 42.6)	26.3 (19.2, 42.5)	28.5 (17.3, 42.9)	0.980
caFFR	0.93 (0.90, 0.95)	0.93 (0.91, 0.95)	0.92 (0.88, 0.96)	0.229
Echocardiographic parameters				
LVEF, %	51.0 ± 7.6	51.3 ± 7.3	50.1 ± 8.4	0.412
LVEDD, mm	47.8 ± 4.7	47.7 ± 4.7	48.4 ± 4.9	0.428

Values are median (IQR), n (%), or mean ± SD.

Abbreviations: ACEI, angiotensin-converting enzyme inhibitor; ARB, angiotensin receptor blocker; ARNI, angiotensin receptor/neprilysin inhibitor; BMI, body mass index; BNP, brain natriuretic peptide; caFFR, coronary angiography-derived fractional flow reserve; caIMR, coronary angiography-derived index of microcirculatory resistance; eGFR, estimated glomerular filtration rate; hs-CRP, high-sensitivity C-reactive protein; IQR, inter-quartile range; LAD, left anterior descending; LCX, left circumflex artery; LVEDD, left ventricular end-diastolic diameter; LVEF, left ventricular ejection fraction; MRA, mineralocorticoid receptor antagonist; PCI, percutaneous coronary intervention; RCA, right coronary artery; SD, standard deviation; TIMI, thrombolysis in myocardial infarction.

(p = 0.0408 and 0.0472, respectively), indicating that incorporating CMR or functional parameters into the clinical model can significantly improve the prediction ability of LVR. There was no significant difference between model 2 and model 3 (p = 0.7401).

Feature importance

To identify important features in Model 2 and Model 3, we performed a feature importance plot using SHAP values and listed the features in descending order. The top three important features in Model 2 were infarct size, MVO, and hemoglobin at admission, which contributed to higher predictive powers than the bottom features (Figure 3A), and that a higher infarct size and the presence of MVO indicate a greater likelihood of LVR. Similarly, the top three important features in Model 3 were current smoking, caFFR, and hemoglobin at admission, contributing to higher predictive powers than the bottom features (Figure 3B), and a lower caFFR indicates a greater likelihood of LVR.

DISCUSSION

In this study, we aimed to develop and evaluate machine learning models for predicting LVR in patients with STEMI undergoing primary PCI. The results demonstrated that incorporating CMR or coronary functional parameters into the clinical model significantly improved the ability to predict LVR, with no significant difference between the two models. This suggests that functional parameters, such as caFFR and caIMR, can effectively replace CMR parameters in predicting LVR, overcoming the limitations of CMR application in patients with STEMI.

The study identified several important factors associated with LVR, such as infarct size, MVO, and hemoglobin levels at admission. Our findings are consistent with previous studies that reported that larger infarct sizes and the presence of MVO were associated with a higher risk of LVR.[18,19] Hemoglobin levels at admission have been reported to be associated with cardiovascular outcomes in patients with ST-segment elevation myocardial infarction (STEMI), with lower levels associated with an increased risk of adverse events, including LVR.[20,21] Our study further supports the importance of these factors in predicting LVR, which may help clinicians identify high-risk patients and optimize their management.

Identifying high-risk individuals allows the prompt initiation of pharmacological agents, such as angiotensin receptor neprilysin inhibitors (ARNI) and sodium-glucose cotransporter-2 inhibitors (SGLT2i), to mitigate LVR.[22,23] They emphasize the need for intensified clinical surveillance of identified high-risk patients and advocate regular follow-up according to evidence-based practices for individuals at increased risk of adverse prognosis. In addition, the study demonstrated that functional parameters such as caFFR and caIMR could effectively replace CMR

Table 2. Cardiac magnetic resonance characteristics of the study population

	Overall (n = 157)	No remodeling (n = 120)	Remodeling (n = 37)	*p* value
CMR findings at index admission				
Intervals, day	3.6 (2.7, 4.6)	3.7 (2.8, 4.6)	3.5 (2.6, 4.4)	0.234
LVEF, %	50.1 ± 11.5	51.4 ± 11.3	46.2 ± 11.2	0.016
LVEDVi, mL/m^2	68.6 ± 14.1	69.8 ± 13.4	64.8 ± 15.8	0.061
LVESVi, mL/m^2	34.5 ± 11.7	34.3 ± 11.6	35.2 ± 12.2	0.671
GLS, %	−8.7 ± 3.2	−9.0 ± 3.1	−7.4 ± 3.2	0.007
The area at risk, % LV mass	63.3 (54.9, 69.7)	62.4 (54.6, 67.7)	65.8 (55.7, 71.8)	0.191
Presence of IMH	54 (36.0%)	36 (31.3%)	18 (51.4%)	0.030
Infarct size, % LV mass	36.2 (28.6, 43.0)	34.78 (25.9, 38.8)	41.5 (32.9, 49.5)	0.001
Presence of MVO	84 (53.4%)	59 (49.2%)	25 (67.6%)	0.050
CMR findings at follow-up				
Intervals, day	106.0 (92.0, 135.0)	106.0 (90.5, 141.3)	106.0 (92.5, 121.0)	0.352
LVEF, %	55.1 ± 10.3	56.6 ± 9.5	50.2 ± 11.1	0.001
LVEDVi, mL/m^2	73.1 ± 16.7	69.2 ± 13.6	85.4 ± 19.7	<0.001
LVESVi, mL/m^2	33.8 ± 14.1	30.7 ± 11.1	43.8 ± 17.9	<0.001
GLS, %	−10.1 ± 3.2	−10.6 ± 2.9	−8.8 ± 3.8	0.004
Infarct size, % LV mass	25.5 (18.0, 33.9)	23.6 (17.0, 32.4)	32.6 (23.6, 40.1)	0.002

Values are median (IQR), n (%), or mean ± SD.

Abbreviations: GLS, global longitudinal strain; IMH, intra-myocardial hemorrhage; IQR, inter-quartile range; LVEDVi, left ventricular end-diastolic volume index; LVEF, left ventricular ejection fraction; LVESVi, left ventricular end-systolic volume index; MVO, microvascular obstruction; SD, standard deviation.

parameters for LVR prediction. In the context of predicting adverse remodeling in patients with STEMI, previous investigations have relied heavily on CMR imaging features such as myocardial strain, MVO, and infarct size.[9,24–26] However, the widespread use of CMR is hampered by the need for contrast agents and the presence of contraindications. Coronary angiography is essential for patients with STEMI undergoing PPCI and plays a crucial role in guiding interventions and assessing coronary artery involvement, as highlighted in the guidelines for the management of acute coronary syndromes.[27] These angiography-derived coronary functional indices can potentially provide a more convenient and accessible way to assess coronary lesions and microcirculatory function, reducing the risks and complexities associated with invasive measurements. Furthermore, both coronary angiography and echocardiographic parameters are widely recognized for their widespread use and clinical applicability in routine practice. Our study addresses these limitations by pioneering a paradigm shift, replacing traditional CMR indicators with coronary angiography and echocardiographic parameters. This strategic change not only maintained comparable predictive value, but also introduced a more clinically feasible and accessible approach. Furthermore, the existing literature firmly establishes a significant correlation between caIMR and pathological evolution after acute myocardial infarction.[28] This foundational relationship fortifies the theoretical underpinning of our study, substantiating the strategic use of caIMR in predicting LVR. This fundamental relationship strengthens the theoretical underpinning of our study and supports the strategic use of caIMR in predicting LVR. This finding is particularly relevant in the context of patients with STEMI for whom CMR may be difficult or contraindicated. The use of caFFR and caIMR may help to identify high-risk patients and guide therapeutic decisions.

Our study used machine learning algorithms to develop prediction models for LVR, which have several advantages over traditional statistical methods. ML models can handle complex interactions and nonlinear relationships between variables and are less influenced by established parameters.[29] This allows for the discovery of innovative predictors and the identification of important features that may have been missed in previous studies.[30] In addition, ML models can be continuously updated and improved as new data becomes available, potentially increasing their predictive accuracy over time. These features make ML models a promising tool for clinical risk prediction and decision making in cardiovascular medicine.

As we consider the future trajectory of this research, several promising avenues emerge. First and foremost, the validation of our models with larger and more diverse sample sizes will be instrumental in strengthening the reliability and applicability of our predictive frameworks. In addition, extending the follow-up period in subsequent studies is imperative to assess the long-term predictive accuracy and stability of our models. Furthermore, given the dynamic nature of medical research, the exploration of additional variables or parameters beyond those included in the current study may help refine and expand the predictive capabilities of our models. Future research efforts will benefit from a comprehensive investigation of these aspects, paving the way for a deeper understanding of the predictive factors associated with our proposed models. In summary, the evolution of this research will involve a concerted effort toward validation, long-term evaluation, and the exploration of innovative variables that will collectively contribute to the advancement of predictive modeling in our field.

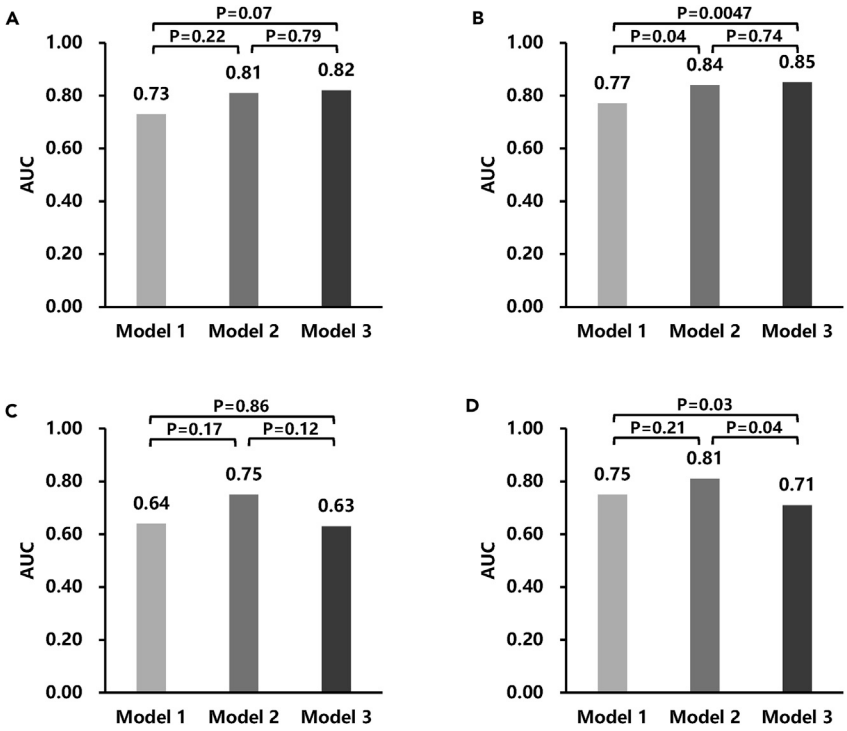

Figure 2. Comparison of the predictive ability of the models

Four machine learning algorithms, including Extreme Gradient Boosting (XGBoost, Figure 2A), K-nearest neighbors (KNN, Figure 2B), logistic regression (LR, Figure 2C), and random forest (RF, Figure 2D), were conducted to construct the predictive model for 3-month LVR and performance was evaluated by area under the receiver operating characteristic curve (AUC).

Our study results suggest that the combination of CMR-based ischemia- and deformation-related indices or coronary physiological measurements with echocardiographic parameters can both effectively predict LVR at 3 months in patients with STEMI undergoing PPCI. Coronary physiological parameters such as caFFR and caIMR have the potential to replace CMR parameters and provide more convenient and reliable methods to assess LVR. These results have important implications for identifying patients with high-risk heart failure and optimizing their management. Further studies with larger sample sizes and longer follow-up are needed to validate and extend our findings.

Limitations of the study

Our study has several limitations. First, the sample size was relatively small, which may have limited the power to detect significant associations and differences between models. Future studies with larger sample sizes are warranted to validate our findings. Second, although our investigation was conducted at a single center, the use of a prospective consecutive enrollment strategy helped to mitigate selection bias. However, we recognize the inherent limitations of generalizing findings from a single center. To address this, future research will include multicenter studies to validate and extend our findings to diverse patient populations. Finally, we only evaluated the performance of the models at 3 months, and the predictive accuracy of the models for longer-term outcomes remains to be evaluated.

STAR★METHODS

Detailed methods are provided in the online version of this paper and include the following:

- KEY RESOURCES TABLE
- RESOURCE AVAILABILITY
  - Lead contact
  - Materials availability
  - Data and code availability
- EXPERIMENTAL MODEL AND STUDY PARTICIPANT DETAILS
  - Study population

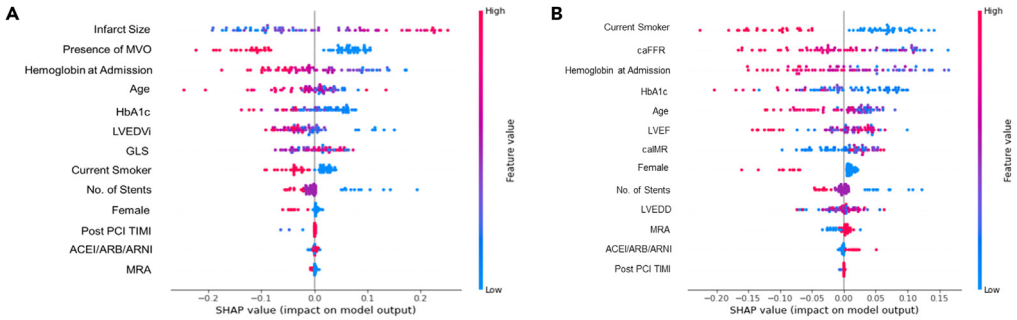

Figure 3. SHAP Analysis of Important Features in the Random Forest Model

The SHAP summary plot (Figure 3) integrates feature importance and individual feature values. Each point represents a sample, with the y axis indicating the feature and the x axis representing the corresponding SHAP value. Redder hues indicate larger feature values, while bluer tones represent smaller values. In Model 2 (Figure 3A), the top three important features were infarct size, MVO (microvascular obstruction), and hemoglobin at admission, associated with a higher likelihood of LVR. In Model 3 (Figure 3B), the top three important features were current smoking, caFFR (coronary artery fractional flow reserve), and hemoglobin at admission, with a lower caFFR indicating a higher likelihood of LVR. The SHAP analysis provides insights into the relationship between features and LVR predictions. Abbreviations: ACEI, angiotensin-converting enzyme inhibitor; ARB, angiotensin receptor blocker; ARNI, angiotensin receptor/neprilysin inhibitor; caFFR, coronary angiography-derived fractional flow reserve; caIMR, coronary angiography-derived index of microcirculatory resistance; GLS, global longitudinal strain; LVEDD, left ventricular end-diastolic diameter; LVEF, left ventricular ejection fraction; MRA, mineralocorticoid receptor antagonist; MVO, microvascular obstruction; PCI, percutaneous coronary intervention; TIMI, thrombolysis in myocardial infarction.

SUPPLEMENTAL INFORMATION

Supplemental information can be found online at https://doi.org/10.1016/j.isci.2024.109513.

ACKNOWLEDGMENTS

This study was funded by grants from the Beijing Hospitals Authority Youth Programme (QLM20230608), the National Key R&D Program of China (2022YFC2505600), and the Training Program for Outstanding Young Scholars in Beijing Anzhen Hospital, Capital Medical University (AZ2023-YQ-03). Dr. Shaoping Nie: research grants to the institution from Boston Scientific, Abbott, Jiangsu Hengrui Pharmaceuticals, China Resources Sanjiu Medical & Pharmaceuticals, and East China Pharmaceuticals. The rest of the authors have no relevant relationships to disclose.

AUTHOR CONTRIBUTIONS

Study concept and design: WZ and QG. Acquisition, analysis, or interpretation of data: QG, RG, YG, HW, LX, HA, and BQ. Drafting of the article: WZ and QG. Statistical review of the article: WZ, QG, RG, YG, HW, and XW. Critical revision of the article for important intellectual content: XW and SN. All authors read and approved the final article.

DECLARATION OF INTERESTS

All authors declare that they have no conflicts of interest.

Received: September 18, 2023
Revised: January 30, 2024
Accepted: March 13, 2024
Published: March 15, 2024

REFERENCES

1. Zile, M.R., Gaasch, W.H., Patel, K., Aban, I.B., and Ahmed, A. (2014). Adverse left ventricular remodeling in community-dwelling older adults predicts incident heart failure and mortality. JACC Heart Fail. *2*, 512–522. https://doi.org/10.1016/j.jchf.2014.03.016.
2. Barnett, R. (2019). Acute myocardial infarction. Lancet *393*, 2580. https://doi.org/10.1016/S0140-6736(19)31419-9.
3. van der Bijl, P., Abou, R., Goedemans, L., Gersh, B.J., Holmes, D.R., Jr., Ajmone Marsan, N., Delgado, V., and Bax, J.J. (2020). Left Ventricular Post-Infarct Remodeling: Implications for Systolic Function Improvement and Outcomes in the Modern Era. JACC Heart Fail. *8*, 131–140. https://doi.org/10.1016/j.jchf.2019.08.014.
4. van den Borne, S.W.M., Diez, J., Blankesteijn, W.M., Verjans, J., Hofstra, L., and Narula, J. (2010). Myocardial remodeling after infarction: the role of myofibroblasts. Nat. Rev. Cardiol. *7*, 30–37. https://doi.org/10.1038/nrcardio.2009.199.
5. Cokkinos, D.V., and Belogianneas, C. (2016). Left Ventricular Remodelling: A Problem in Search of Solutions. Eur. Cardiol. *11*, 29–35. https://doi.org/10.15420/ecr.2015:9:3.
6. Bulluck, H., Dharmakumar, R., Arai, A.E., Berry, C., and Hausenloy, D.J. (2018). Cardiovascular Magnetic Resonance in Acute ST-Segment-Elevation Myocardial Infarction: Recent Advances, Controversies, and Future Directions. Circulation *137*, 1949–1964. https://doi.org/10.1161/CIRCULATIONAHA.117.030693.
7. Ibanez, B., Aletras, A.H., Arai, A.E., Arheden, H., Bax, J., Berry, C., Bucciarelli-Ducci, C., Croisille, P., Dall'Armellina, E., Dharmakumar, R., et al. (2019). Cardiac MRI Endpoints in Myocardial Infarction Experimental and Clinical Trials: JACC Scientific Expert Panel. J. Am. Coll. Cardiol. *74*, 238–256. https://doi.org/10.1016/j.jacc.2019.05.024.
8. Mangion, K., McComb, C., Auger, D.A., Epstein, F.H., and Berry, C. (2017). Magnetic Resonance Imaging of Myocardial Strain After Acute ST-Segment-Elevation Myocardial Infarction: A Systematic Review. Circ. Cardiovasc. Imag. *10*. https://doi.org/10.1161/CIRCIMAGING.117.006498.
9. Reindl, M., Tiller, C., Holzknecht, M., Lechner, I., Eisner, D., Riepl, L., Pamminger, M., Henninger, B., Mayr, A., Schwaiger, J.P., et al. (2021). Global longitudinal strain by feature tracking for optimized prediction of adverse remodeling after ST-elevation myocardial infarction. Clin. Res. Cardiol. *110*, 61–71. https://doi.org/10.1007/s00392-020-01649-2.
10. Masci, P.G., Ganame, J., Francone, M., Desmet, W., Lorenzoni, V., Iacucci, I., Barison, A., Carbone, I., Lombardi, M., Agati, L., et al. (2011). Relationship between location and size of myocardial infarction and their reciprocal influences on post-infarction left ventricular remodelling. Eur. Heart J. *32*, 1640–1648. https://doi.org/10.1093/eurheartj/ehr064.
11. Orn, S., Manhenke, C., Anand, I.S., Squire, I., Nagel, E., Edvardsen, T., and Dickstein, K. (2007). Effect of left ventricular scar size, location, and transmurality on left ventricular remodeling with healed myocardial infarction. Am. J. Cardiol. *99*, 1109–1114. https://doi.org/10.1016/j.amjcard.2006.11.059.
12. Hamirani, Y.S., Wong, A., Kramer, C.M., and Salerno, M. (2014). Effect of microvascular obstruction and intramyocardial hemorrhage by CMR on LV remodeling and outcomes after myocardial infarction: a systematic review and meta-analysis. JACC Cardiovasc. Imag. *7*, 940–952. https://doi.org/10.1016/j.jcmg.2014.06.012.
13. Del Buono, M.G., Montone, R.A., Camilli, M., Carbone, S., Narula, J., Lavie, C.J., Niccoli, G., and Crea, F. (2021). Coronary Microvascular Dysfunction Across the Spectrum of Cardiovascular Diseases: JACC State-of-the-Art Review. J. Am. Coll. Cardiol. *78*, 1352–1371. https://doi.org/10.1016/j.jacc.2021.07.042.
14. Hong, D., Lee, S.H., Shin, D., Choi, K.H., Kim, H.K., Ha, S.J., Joh, H.S., Park, T.K., Yang, J.H., Song, Y.B., et al. (2023). Prognostic Impact of Cardiac Diastolic Function and Coronary Microvascular Function on Cardiovascular Death. J. Am. Heart Assoc. *12*, e027690. https://doi.org/10.1161/JAHA.122.027690.
15. Li, J., Gong, Y., Wang, W., Yang, Q., Liu, B., Lu, Y., Xu, Y., Huo, Y., Yi, T., Liu, J., et al. (2020). Accuracy of computational pressure-fluid dynamics applied to coronary angiography to derive fractional flow reserve: FLASH FFR. Cardiovasc. Res. *116*, 1349–1356. https://doi.org/10.1093/cvr/cvz289.
16. Zhou, Z., Zhu, B., Fan, F., Yang, F., Fang, S., Wang, Z., Qiu, L., Gong, Y., and Huo, Y. (2022). Prognostic Value of Coronary Angiography-Derived Fractional Flow Reserve Immediately After Stenting. Front. Cardiovasc. Med. *9*, 834553. https://doi.org/10.3389/fcvm.2022.834553.
17. Jamin, A., Abraham, P., and Humeau-Heurtier, A. (2021). Machine learning for predictive data analytics in medicine: A review illustrated by cardiovascular and nuclear medicine examples. Clin. Physiol. Funct. Imag. *41*, 113–127. https://doi.org/10.1111/cpf.12686.
18. Gerber, B.L., Rochitte, C.E., Melin, J.A., McVeigh, E.R., Bluemke, D.A., Wu, K.C., Becker, L.C., and Lima, J.A. (2000). Microvascular obstruction and left ventricular remodeling early after acute myocardial infarction. Circulation *101*, 2734–2741. https://doi.org/10.1161/01.cir.101.23.2734.
19. Wu, K.C. (2012). CMR of microvascular obstruction and hemorrhage in myocardial infarction. J. Cardiovasc. Magn. Reson. *14*, 68. https://doi.org/10.1186/1532-429X-14-68.
20. Dutsch, A., Graesser, C., Voll, F., Novacek, S., Eggerstedt, R., Armbruster, N.L., Laugwitz, K.L., Cassese, S., Schunkert, H., Ndrepepa, G., et al. (2022). Association of In-Hospital Hemoglobin Drop With Decreased Myocardial Salvage and Increased Long-Term Mortality in Patients With Acute ST-Segment-Elevation Myocardial Infarction. J. Am. Heart Assoc. *11*, e024857. https://doi.org/10.1161/JAHA.121.024857.
21. Gao, M., Zhang, X., Qin, L., Zheng, Y., Zhang, Z., Tong, Q., and Li, H. (2020). Discharge Hemoglobin Association with Long-Term Outcomes of ST-Elevation Myocardial Infarction Patients Undergoing Primary Percutaneous Coronary Intervention. Cardiovasc. Ther. *2020*, 8647837. https://doi.org/10.1155/2020/8647837.
22. Shah, A.M., Claggett, B., Prasad, N., Li, G., Volquez, M., Jering, K., Cikes, M., Kovacs, A., Mullens, W., Nicolau, J.C., et al. (2022). Impact of Sacubitril/Valsartan Compared With Ramipril on Cardiac Structure and Function After Acute Myocardial Infarction: The PARADISE-MI Echocardiographic Substudy. Circulation *146*, 1067–1081. https://doi.org/10.1161/CIRCULATIONAHA.122.059210.
23. von Lewinski, D., Kolesnik, E., Tripolt, N.J., Pferschy, P.N., Benedikt, M., Wallner, M., Alber, H., Berger, R., Lichtenauer, M., Saely, C.H., et al. (2022). Empagliflozin in acute myocardial infarction: the EMMY trial. Eur. Heart J. *43*, 4421–4432. https://doi.org/10.1093/eurheartj/ehac494.
24. Bodi, V., Monmeneu, J.V., Ortiz-Perez, J.T., Lopez-Lereu, M.P., Bonanad, C., Husser, O., Minana, G., Gomez, C., Nunez, J., Forteza, M.J., et al. (2016). Prediction of Reverse Remodeling at Cardiac MR Imaging Soon after First ST-Segment-Elevation Myocardial Infarction: Results of a Large Prospective Registry. Radiology *278*, 54–63. https://doi.org/10.1148/radiol.2015142674.
25. Calvieri, C., Riva, A., Sturla, F., Dominici, L., Conia, L., Gaudio, C., Miraldi, F., Secchi, F., and Galea, N. (2023). Left Ventricular Adverse Remodeling in Ischemic Heart Disease: Emerging Cardiac Magnetic Resonance Imaging Biomarkers. J. Clin. Med. *12*, 334. https://doi.org/10.3390/jcm12010334.
26. Hamirani, Y.S., Wong, A., Kramer, C.M., and Salerno, M. (2014). Effect of microvascular obstruction and intramyocardial hemorrhage by CMR on LV remodeling and outcomes after myocardial infarction: a systematic review and meta-analysis. JACC Cardiovasc. Imag. *7*, 940–952. https://doi.org/10.1016/j.jcmg.2014.06.012.
27. Byrne, R.A., Rossello, X., Coughlan, J.J., Barbato, E., Berry, C., Chieffo, A., Claeys, M.J., Dan, G.A., Dweck, M.R., Galbraith, M., et al. (2023). 2023 ESC Guidelines for the management of acute coronary syndromes. Eur. Heart J. *44*, 3720–3826. https://doi.org/10.1093/eurheartj/ehad191.
28. Wang, X., Guo, Q., Guo, R., Guo, Y., Yan, Y., Gong, W., Zheng, W., Wang, H., Ai, H., Que, B., et al. (2023). Coronary angiography-derived index of microcirculatory resistance and evolution of infarct pathology after ST-segment-elevation myocardial infarction. Eur. Heart J. Cardiovasc. Imaging *24*, 1640–1652. https://doi.org/10.1093/ehjci/jead141.
29. Durmaz, E.S., Karabacak, M., Ozkara, B.B., Kargın, O.A., Raimoglu, U., Tokdil, H., Durmaz, E., and Adaletli, I. (2023). Radiomics-based machine learning models in STEMI: a promising tool for the prediction of major adverse cardiac events. Eur. Radiol. *33*, 4611–4620. https://doi.org/10.1007/s00330-023-09394-6.
30. Zhang, W., Singh, S., Liu, L., Mohammed, A.Q., Yin, G., Xu, S., Lv, X., Shi, T., Feng, C., Jiang, R., et al. (2022). Prognostic value of coronary microvascular dysfunction assessed by coronary angiography-derived index of microcirculatory resistance in diabetic patients with chronic coronary syndrome. Cardiovasc. Diabetol. *21*, 222. https://doi.org/10.1186/s12933-022-01653-y.
31. Thygesen, K., Alpert, J.S., Jaffe, A.S., Chaitman, B.R., Bax, J.J., Morrow, D.A.,

and White, H.D.; Executive Group on behalf of the Joint European Society of Cardiology ESC/American College of Cardiology ACC/American Heart Association AHA/World Heart Federation WHF Task Force for the Universal Definition of Myocardial Infarction (2018). Fourth Universal Definition of Myocardial Infarction (2018). J. Am. Coll. Cardiol. *72*, 2231–2264. https://doi.org/10.1016/j.jacc.2018.08.1038.

32. Ai, H., Feng, Y., Gong, Y., Zheng, B., Jin, Q., Zhang, H.P., Sun, F., Li, J., Chen, Y., Huo, Y., and Huo, Y. (2020). Coronary Angiography-Derived Index of Microvascular Resistance. Front. Physiol. *11*, 605356. https://doi.org/10.3389/fphys.2020.605356.

33. Zhao, E., Xie, H., and Zhang, Y. (2020). Predicting Diagnostic Gene Biomarkers Associated With Immune Infiltration in Patients With Acute Myocardial Infarction. Front. Cardiovasc. Med. *7*, 586871. https://doi.org/10.3389/fcvm.2020.586871.

34. Cavallo, A.U., Troisi, J., Muscogiuri, E., Cavallo, P., Rajagopalan, S., Citro, R., Bossone, E., McVeigh, N., Forte, V., Di Donna, C., et al. (2022). Cardiac Computed Tomography Radiomics-Based Approach for the Detection of Left Ventricular Remodeling in Patients with Arterial Hypertension. Diagnostics *12*, 322. https://doi.org/10.3390/diagnostics12020322.

STAR★METHODS

KEY RESOURCES TABLE

REAGENT or RESOURCE	SOURCE	IDENTIFIER
Software and algorithms		
CVI42 (version 5.13)	Circle Cardiovascular Imaging Software	https://www.circlecvi.com
Python (version 3.7)	Python Software Foundation	https://www.python.org
SPSS (version 26.0)	IBM SPSS software	https://www.ibm.com
R (version 4.1.2)	R software	http://www.R-project.org

RESOURCE AVAILABILITY

Lead contact

Further information and requests for resources should be directed to and will be fulfilled by the lead contact, Xiao Wang (e-mail: xwang@mail.ccmu.edu.cn).

Materials availability

This study did not generate new unique reagents.

Data and code availability

- All data reported in this paper will be shared by the lead contact upon request.
- This paper does not report original code.
- Any additional information required to reanalyze the data reported in this paper is available from the lead contact upon request.

EXPERIMENTAL MODEL AND STUDY PARTICIPANT DETAILS

Study population

Patients with ST-segment elevation myocardial infarction (STEMI) undergoing primary percutaneous coronary intervention (PPCI) admitted to Beijing Anzhen Hospital, Capital Medical University, were prospectively enrolled between October 2019 and August 2021. Inclusion criteria involved patients who underwent cardiac magnetic resonance (CMR) at index admission (3–7 days after PPCI) and follow-up (3 months). STEMI was defined according to the fourth universal definition of myocardial infarction.[31] Exclusion criteria encompassed contraindications to CMR, clinical instability, claustrophobia, reinfarction or death before follow-up CMR, and incomplete CMR studies or poor image quality. Left ventricular remodeling (LVR) was defined as left ventricular end-diastolic volume (LVEDV) equal to or greater than 20% between baseline CMR and the 3-month follow-up.[3] The demographic and clinical characteristics of the participants were shown in Table 1. Information related to patient sex and age can be found in Table 1. Information related to ancestry, race, or ethnicity were not recorded in this study.

Standard protocol approvals, registrations, and patient consents

All subjects provided written informed consent before enrollment, and the institutional review board of Beijing Anzhen Hospital approved this study.

METHOD DETAILS

CMR analysis

CMR was performed on a 3.0-Tesla system (Ingenia CX, Philips Healthcare, Best, The Netherlands, or MR750W, General Electric Healthcare, Waukesha, Wisconsin, USA) using a cine sequence, black blood fat-suppressed T2-weighted (T2w), and late gadolinium enhancement (LGE) imaging protocol. Two professional operators (QG and RG) with three years of experience in CMR image interpretation analyzed all CMR images blindly, and a professional CMR radiologist (HW) reviewed them. CMR data were analyzed using CVI42 software version 5.13 (Circle Cardiovascular Imaging, Calgary, AB, Canada). Borders of the endocardium and epicardium were delineated on contiguous short-axis slices, with cardiac structural and functional indexes quantified from cine images. Myocardial strain analyses involved outlining the endocardial and epicardial borders of the LV at end-diastole in short-axis, two-chamber, three-chamber, and four-chamber tissue, with anterior and inferior insertion points drawn manually. Global longitudinal strain (GLS) was calculated as the software's mean of the respective 16-segment peak values. In LGE images, infarcted tissue was defined as five standard deviations (SDs) above the mean signal intensity of the remote normal myocardium. Hypo-enhancement area within infarcted myocardium represented microvascular obstruction (MVO). Area at risk

(AAR), was identified as enhancement within the myocardium of signal intensity >2 SDs of the mean signal in remote healthy myocardium. Intramyocardial hemorrhage (IMH) was defined as hypo-enhancement within AAR. Infarct size, MVO, and IMH were presented as a percentage of LV end-diastolic mass (%LV mass).

Coronary physiological measurements

Coronary angiography was performed from multiple views and recorded at a frame rate of 15 frames per second. For both angiography-derived fractional flow reserve (caFFR) and index of microcirculatory resistance (caIMR) calculations, at least two angiographic projections were obtained, ensuring avoidance of vessel overlap and having a separation angle of $\geq 30°$. Simultaneously, aortic pressure was recorded using a specialized pressure transducer connected to the guiding catheter. The recorded aortic pressure waveforms and the Digital Imaging and Communications in Medicine (DICOM) images were input into the FlashAngio console, enabling the generation of a three-dimensional (3D) mesh reconstruction of the coronary arteries.

For the calculation of caFFR,[16] resting flow velocities were determined using the Thrombolysis In Myocardial Infarction (TIMI) Frame Count method. Flow velocity data and mean arterial pressure (MAP) obtained from the FlashAngio software were then utilized by a proprietary computational fluid dynamics (CFD) method to compute the pressure drop along the generated mesh of the coronary artery, thereby enabling the calculation of caFFR.

$$caFFR = \frac{P_d}{P_a}$$

Where P_d represents the pressure at the distal end of the coronary artery, P_a is the aortic pressure, which is typically the pressure at the entrance of the coronary artery. The pressures P_a and P_d are obtained from the CFD analysis based on the angiographic data and aortic pressure waveform. The CFD method uses resting flow velocities (determined by the TIMI Frame Count method) to compute the pressure drop along the coronary artery mesh, which then helps in determining P_d.

In the case of caIMR,[32] diastolic flow velocity ($V_{diastole}$) was determined using the TIMI Frame Count method. The maximal hyperemic flow velocity (V_{hyp}) was assumed to be 2.1 times the $V_{diastole}$. The CFD method with an inlet velocity of V_{hyp} was employed to compute the pressure drop and calculate caIMR.

$$caIMR = \frac{(P_d)_{hyp} \times L}{K \times V_{diastole}}$$

Where $(P_d)_{hyp}$ is the estimated hyperemic coronary artery pressure, L is a constant representing the length from the inlet to the distal position, K is the constant for flow velocity adjustment (≈ 2.1), $V_{diastole}$ and is the diastolic flow velocity determined using the TIMI Frame Count method.

Both caIMR and caFFR calculations were performed in a blinded manner, without access to the information of the hospital operators. Offline analyses were conducted by an independent core laboratory at Suzhou RainMed Medical Technology Co., Ltd.

Feature selection

The structured dataset included 35 variables, which encompassed 14 clinical variables (age, gender, body mass index [BMI], current smoking, systolic blood pressure at admission, anterior myocardial infarction, HbA1c, neutrophil percentage [NE%], high-sensitivity C-reactive protein, hemoglobin, estimated glomerular filtration rate [eGFR]); three medication variables (treatment with mineralocorticoid-receptor antagonist [MRA], beta-blocker, angiotensin-converting-enzyme inhibitor [ACEI], angiotensin-receptor antagonist [ARB], or angiotensin-receptor neprilysin inhibitor [ARNI]); four angiographic variables (total ischemic time, culprit vessel, TIMI flow grade pre/post-PCI for culprit vessel); two procedural variables (thrombus aspiration and number of stents); two coronary functional indices (caIMR and caFFR); seven CMR features (LVEDVi, LVESVi, left ventricular ejection fraction (LVEF), infarct size, MVO, IMH, and GLS); and two echocardiographic parameters (LVEF and left ventricular end-diastolic diameter [LVEDD]). Missing values were imputed using appropriate imputation methods. LASSO[33] and BORUTA[34] were applied in combination for feature selection, involving the integration of these methods to identify relevant features, followed by an assessment of the clinical significance of each selected feature.

QUANTIFICATION AND STATISTICAL ANALYSIS

Machine learning algorithm and statistical analysis

Continuous variables are presented as median (interquartile range) and categorical variables as number (percentage). Despite the prospective nature of this study, the very low rate of missing data underscores meticulous data collection procedures and stringent quality control, ensuring dataset robustness and reliability. In the preprocessing phase, missing values were initially imputed using the k-nearest neighbor (KNN) algorithm to maximize dataset completeness for machine learning applications. Additionally, a script addressed missing values across continuous, unordered categorical, and ordered categorical variable types via tailored strategies including mean, mode, and median imputation respectively. This comprehensive framework integrated KNN-based imputation of clinical variables with type-specific handling, optimizing the final dataset. To address the imbalanced dataset, we applied the Synthetic Minority Over-sampling Technique (SMOTE) to generate synthetic samples for the minority class, effectively balancing classes. Using the original feature matrix (X) and labels (y), SMOTE

produced new feature (X_resampled) and label (y_resampled) arrays encompassing both real and synthetic samples. This proved instrumental in enabling high-performance models. The full dataset was then randomly divided into 70% training and 30% validation subsets. Machine learning methods employed were XGBoost, logistic regression (LR), KNN, and random forest (RF). Model performance was evaluated via area under receiver operating characteristic curve (AUC) and precision-recall curves using the Delong test for comparisons. SHapley Additive exPlanations (SHAP) provided accurate feature attribution values. Analysis was conducted in Python 3.7, R 4.1.2 and SPSS 26.0, with two-tailed $p < 0.05$ indicating significance.